dependence of the reconstruction accuracy on the size of the scatterer under test. Moreover, some investigations will be devoted to studying the matching between the multistep procedure and iterative statistical minimization methods in order to reduce the computational load (minimizing at each step the number of unknowns), exploiting the robustness in terms of the capability to reach global minima. To this end, a version of the approach hybridized with a genetic algorithm is currently under development.

## REFERENCES

1. J.C. Bolomey, Recent European development in active microwave imaging for industrial, scientific and medical applications, IEEE Trans Microwave Theory Tech 37 (1989), 2109–2117.
2. R. Zoughi, Microwave nondestructive testing and evaluation, Kluwer Academic, The Netherlands, 2000.
3. M. Bertero and P. Boccacci, Inverse problems in imaging, IOP Publishing, Bristol, England, 1998.
4. M. Azimi and A.C. Kak, Distortion in diffraction tomography caused by multiple scattering, IEEE Trans Med Imaging MI-2 (1983), 176–195.
5. R. Maini, M.F. Iskander, and C.H. Durney, On electromagnetic imaging using linear reconstruction techniques, Proc IEEE 68 (1980), 1550–1552.
6. M. Slaney, A.C. Kak, and L.E. Larsen, Limitation of imaging with first order diffraction tomography, IEEE Trans Microwave Theory Tech MTT-32 (1984), 860–874.
7. W.C. Chew and Y.M. Wang, Reconstruction of two-dimensional permittivity distribution using the distorted Born iterative method, IEEE Trans Med Imaging 9 (1990), 218–225.
8. K. Belkebir, R.E. Kleinman, and C. Pichot, Microwave imaging location and shape reconstruction from multifrequency scattering data, IEEE Trans Microwave Theory Tech 45 (1997), 469–476.
9. H. Harada, D.J.N. Wall, T.T. Takenaka, and T. Tanaka, Conjugate gradient method applied to inverse scattering problems, IEEE Trans Antennas Propagat 43 (1995), 784–792.
10. S. Caorsi, A. Massa, and M. Pastorino, A computational technique based on a real-coded genetic algorithm for microwave imaging purposes, IEEE Trans Geosci Remote Sensing (Special issue on Computational wave issues in remote sensing, imaging and target identification, propagation, and inverse scattering) 38 (2000), 1697–1708.
11. S.-Y. Yang, H.-K. Choi, and J.-W. Ra, Reconstruction of a large high-contrast penetrable object by using the genetic and Levenberg-Marquardt algorithms, Microwave Opt Technol Lett 6 (1997), 17–21.
12. O.M. Bucci and T. Isernia, Electromagnetic inverse scattering: Retrievable information and measurement strategies, Radio Sci 32 (1997), 2123–2138.

---

# RESONANT FREQUENCY CALCULATION FOR INHOMOGENEOUS DIELECTRIC RESONATORS USING VOLUME INTEGRAL EQUATIONS AND FACE-CENTERED NODE POINTS

**Keith A. Walters[1] and George W. Hanson[1]**
[1] Department of Electrical Engineering and Computer Science
University of Wisconsin – Milwaukee
Milwaukee, Wisconsin 53211

**ABSTRACT:** *The face-centered node-point technique, developed earlier for scattering applications, is applied to the calculation of resonance frequencies of inhomogeneous dielectric resonators. The described method leads to a well-conditioned matrix system suitable for numerical solution, which is not the case when the permittivity is high and conventional solution techniques (e.g., pulse functions with cell-centered point matching) are employed. In this work, we concentrate on resonators having the shape of a parallelepiped, for which there are relatively few computational results in the literature, although the method can accommodate arbitrarily shaped structures. © 2002 John Wiley & Sons, Inc. Microwave Opt Technol Lett 32: 356–359, 2002.*

## I. INTRODUCTION

Dielectric resonators are typically simple geometric structures (sphere, cylinder, parallelepiped, hemisphere, etc.) fabricated from low-loss, high-permittivity material. They have many applications in high-frequency circuits, such as temperature-compensated oscillators, microwave frequency synthesizers, narrow-bandpass filters [3], and antennas [4]. Resonators that are inhomogeneous and have high permittivity present a difficult challenge for numerical simulation tools, and to our knowledge, no computational results have been presented in the literature for this class of structure. For dielectric resonator antennas, the case of an inhomogeneous, rather than homogeneous, resonator has been found to be useful for impedance-matching [5] and bandwidth-enhancement techniques [6], and similar properties would be expected for other integrated resonator applications. In this work, we present an accurate full-wave method for determining the complex resonance frequencies of inhomogeneous, high-permittivity dielectric resonators using a volume integral-equation technique.

Volume integral equations have been used in the past by many authors to analyze scattering from arbitrarily shaped, inhomogeneous three-dimensional bodies. Typically, the method of moments is utilized to convert the integral equations into a finite matrix equation that can be solved numerically. In the classic point-matching method, the scatterer is divided into cubical cells using a three-dimensional pulse function basis, while delta functions test the field at the center of the cell. Although this method can, in principle, accommodate strongly inhomogeneous media, it is noted that pulse functions are only appropriate for fields that are relatively constant throughout each cell [7–8], requiring large numbers of cells to model complex scatterers. Furthermore, it has been shown that, as the number of cells is increased, the solution may converge to an incorrect answer [9–10] or may fail to converge at all [11–12]. These problems are associated with the improper modeling of polarization charge induced at the interface of dissimilar media, and are exacerbated when the permittivity of the scatterer is high. As this charge term increases, errors in the off-diagonal elements of the method-of-moments matrix, representing coupling between nearby cells, also increases, and the resultant matrix becomes ill conditioned [13–14]. Attempts have been made to model the scatterer using higher order basis functions [12–15] to improve accuracy, but generally, this still does not reduce the sensitivity of the solution to ill-conditioned matrices [2].

The method utilized here is a variation of the point-matching method. Since polarization charges are only induced at the interface between two dissimilar media, the testing functions (delta functions) are placed at the centers of the cubical faces [1–2]. This face-centered node-point method

allows the polarization charge to be modeled more accurately, and the resulting matrix is well conditioned, even for high-permittivity scatterers. Although the method was previously developed for scattering calculations, here we show that it is very well suited for determining the complex resonance frequencies of inhomogeneous dielectric resonators which, in practical applications, are usually constructed from materials having very high permittivities. Resonators in free space are considered to illustrate the method, although other background environments can be accommodated by modifying the Green's function. Because the method is based on a rigorous integral equation technique, higher order resonances can be found using this technique, although in this work, we concentrate on the fundamental resonance. Moreover, the problem of resonator coupling and excitation can be similarly analyzed by incorporating appropriate feed structures, although this topic is not pursued here.

## II. FORMULATION

Consider an incident electric field impinging on an inhomogeneous dielectric resonator having relative permittivity $\varepsilon_r(\vec{r})$ and residing in free space. At any point in space, the total electric field $\vec{E}(\vec{r})$ can be written in terms of the incident electric field $\vec{E}^i(\vec{r})$ and the scattered electric field $\vec{E}^s(\vec{r})$ as $\vec{E}(\vec{r}) = \vec{E}^i(\vec{r}) + \vec{E}^s(\vec{r})$ or

$$\vec{E}(\vec{r}) = \vec{E}^i(\vec{r}) - j\omega\mu_0 \int_V \vec{J}_{\rm eq}(\vec{r}')G(\vec{r},\vec{r}')dV'$$

$$- \frac{1}{\varepsilon_0}\nabla \int_V \rho_{\rm eq}(\vec{r}')G(\vec{r},\vec{r}')dV' \quad (1)$$

where $\vec{J}_{\rm eq}(\vec{r}) = j\omega\varepsilon_0\chi_e(\vec{r})\vec{E}(\vec{r})$ and $\rho_{\rm eq}(\vec{r}) = -\varepsilon_0\nabla \cdot (\chi_e(\vec{r})\vec{E}(\vec{r}))$ are the equivalent polarization current and charge, respectively, $\chi_e(\vec{r}) = (\varepsilon_r(\vec{r}) - 1)$, $G(\vec{r},\vec{r}') = e^{-jk_0R}/4\pi R$ is the free-space Green's function, $k_0 = \omega\sqrt{\mu_0\varepsilon_0}$, $R = |\vec{r} - \vec{r}'|$, and $V$ is the volume of the resonator. The restriction $\vec{r} \in V$ leads to the usual volume integral equation for determining $\vec{E}(\vec{r})$. Writing the above equation entirely in terms of $\vec{E}(\vec{r})$, we obtain

$$\vec{E}(\vec{r}) = \vec{E}^i(\vec{r}) + k_0^2 \int_V G(\vec{r},\vec{r}')\chi_e(\vec{r}')\vec{E}(\vec{r}')dV'$$

$$+ \nabla \int_V G(\vec{r},\vec{r}')\nabla' \cdot (\chi_e(\vec{r}')\vec{E}(\vec{r}'))dV'. \quad (2)$$

In natural resonance problems, we set $\vec{E}^i(\vec{r}) = 0$, and seek nontrivial solutions of the homogeneous integral equation

$$k_0^2(\omega)\int_V G(\vec{r},\vec{r}',\omega)\chi_e(\vec{r}')\vec{E}(\vec{r}',\omega)dV' + \nabla \int_V G(\vec{r},\vec{r}',\omega)$$

$$\cdot \nabla'(\chi_e(\vec{r}')\vec{E}(\vec{r}',\omega))dV' - \vec{E}(\vec{r},\omega) = 0 \quad (3)$$

where we consider the continuation of into the complex $\omega$-plane. The solution of results in the natural resonant frequency $\omega = \omega_{nmp}$ and the associated natural-mode field at resonance $\vec{E}(\vec{r}) = \vec{E}_{nmp}(\vec{r})$.

## III. NUMERICAL PROCEDURE

To solve (2) or (3), we decompose the arbitrarily shaped resonator into $m_x \times m_y \times m_z$ identical rectangular cells (one could also utilize cells of different sizes), each cell having volume $\Delta v = \Delta x \times \Delta y \times \Delta z$. As shown in Figure 1, the
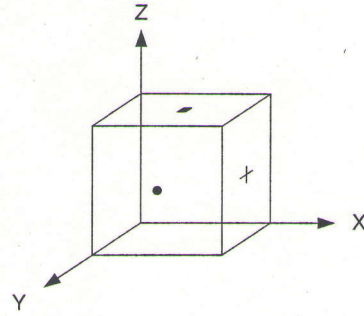


**Figure 1**   Cubic cell with face-centered node points

node points are located on the surfaces of the cells; the cross (+), circle (•), and square (▪) indicate where $E_x$, $E_y$, and $E_z$ are sampled, respectively. Since the node points reside on the cell faces, (2) or (3) must be solved for a body comprised of both the resonator and a one-cell-thick layer of the surrounding space ($\varepsilon_r = 1$) using $M = (m_x + 1) \times (m_y + 1) \times (m_z + 1)$ cells.

When modeling the resonator, the number of cells is chosen so that the electric field and permittivity of each cell are relatively constant. In doing so, the problem of a single heterogeneous body in a nonuniform field is converted into a system of simple homogeneous cells in a quasistatic field. Induced charges will appear only on the surfaces of these "electrically small" homogeneous cells, and can be determined by the normal component of the electric field at each cell face. Placing the node points on the surfaces of the cells gives one the option of choosing to solve for the electric field on either side of the interface. By choosing the appropriate side, we can reduce the magnitude of the off-diagonal matrix elements, and produce a well-conditioned matrix [1–2].

Using the method of moments and applying a pulse function basis with face-centered delta function testing, the integral equation (2) is expressed as a matrix equation of the form $\mathbf{Ax} = \mathbf{b}$, where $\mathbf{A}$ is a $3M \times 3M$ matrix, $\mathbf{x}$ is a $3M$ vector of unknowns, and $\mathbf{b}$ is a $3M$ vector related to the incident field. Details of the procedure can be found in [1–2] and [16], and so will be omitted here. In the case of the resonance problem (3), we solve $\mathbf{A}(\omega)\mathbf{x} = \mathbf{0}$, leading to the equation $\det[\mathbf{A}(\omega)] = 0$. Assuming that the resonant frequency is a simple root of the determinant function, the natural mode field $\vec{E}_{nmp}(\vec{r})$ is obtained by fixing one coefficient in $\mathbf{x}$ and solving for the nontrivial solution of $\mathbf{A}(\omega)\mathbf{x} = \mathbf{0}$.

## IV. RESULTS

Various checks on the accuracy of the numerical algorithm were performed. First, the electric field scattered from various dielectric cylinders was calculated using (2), and compared to the results in [2]. Excellent agreement was found. We then considered resonance frequency calculation using (3).

For dielectric resonators having the shape of a parallelepiped, the electric field of the fundamental resonance is transverse to the z-axis, otherwise known as a $\mathrm{TE}_{11d}^z$ mode, where $0 < d < 1$. We first considered the following three homogeneous cases.

Geometry 1: Dielectric resonator measuring 7.45 mm × 7.45 mm × 2.98 mm with $\varepsilon_r = 79.46$.

Geometry 2: Dielectric resonator measuring 8.60 mm $\times$ 8.60 mm $\times$ 2.58 mm with $\varepsilon_r = 37.84$.

Geometry 3: Dielectric resonator measuring 8.77 mm $\times$ 8.77 mm $\times$ 3.51 mm with $\varepsilon_r = 37.84$.

Each resonator was modeled with $m_x \times m_y \times m_z$ cells in a space of $(m_x + 1) \times (m_y + 1) \times (m_z + 1)$ cells (resonator + air), where $m_x = m_y$. Table 1 represents the convergence data for Geometry 1. The data from all three cases are compared to the results obtained by other authors in Table 2. In this table, FWM indicates a full-wave method, DWM indicates an approximate dielectric waveguide model, and FCNP indicates the face-centered node point method considered in this work.
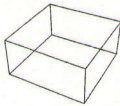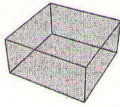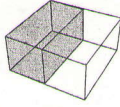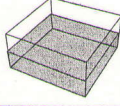
As seen from the above table, results of the face-centered node-point algorithm are in good agreement with the theoretical results computed in [17] (the full-wave method described in [17] is especially well suited to high-permittivity, homogeneous resonators), as well as experimental data collected in [4]. It also provides a significant reduction in error over the results obtained in [4] using a first-order dielectric waveguide model.

Considering inhomogeneous resonators, in Table 3, we compare the resonant frequency of two homogeneous dielectric resonators with two inhomogeneous (multilayered) cases. The homogeneous resonators have relative permittivities $\varepsilon_r = 75$ and $\varepsilon_r = 85$, while the inhomogeneous resonators are comprised of two halves, with one half having relative permittivity $\varepsilon_r = 75$, and the other half $\varepsilon_r = 85$. In the first inhomogeneous case, the boundary between the two materials occurs in the $y-z$ plane halfway along the $x$-axis. In the second case, the boundary occurs in the $x-y$ plane halfway along the $z$-axis. All three resonators have the same dimensional characteristics as Geometry 1 (7.45 mm $\times$ 7.45 mm $\times$ 2.98 mm).

Notice that the resonant frequency of both two-layer dielectric resonators is found to be approximately equal to the average of the resonance frequencies of the two homogeneous resonators.

Since, in Table 3, the inhomogeneous resonators have high permittivities that are fairly similar ($\varepsilon_{r_1} = 85$, $\varepsilon_{r_2} = 75$), to illustrate the flexibility of the method, in Table 4 we consider an inhomogeneous resonator comprised of two homogeneous sections with greatly different permittivities. We also consider the possibility of material loss. The resonator

has dimensions 8.77 mm $\times$ 8.77 mm $\times$ 3.51 mm, and the boundary between the two materials occurs in the $y-z$ plane halfway along the $x$-axis (as in the third entry in Table 3). All results are reported for an $8 \times 8 \times 4$ mesh. Although results for this class of inhomogeneous dielectric resonator are not available in the literature to our knowledge, based on the numerical stability of the algorithm and numerical convergence and field plots, we have high confidence in the presented resonant frequency values. For comparison, note that, for a homogeneous resonator having $\varepsilon_r = 40$, the resonance frequency is $5.506 + 0.0690$ GHz, and if $\varepsilon_r = 45$, the resonance frequency is $5.204 + 0.0559$ GHz.

Other multilayer or generally inhomogeneous arbitrary-shaped resonators can be easily modeled using this technique. Note that the radiation $Q$ for the structures presented, $Q = |F_{\text{res}}|/2 \,\text{Im}(F_{\text{res}})$, is too low for typical resonator applications due to the structure being immersed in free space (although some of the structures may be more suitable for antenna applications). The radiation $Q$ is very sensitive to the

**TABLE 3** Comparison of Homogeneous and Inhomogeneous Dielectric Resoantor Resonant Frequencies

| DR Geometry | $\varepsilon_r$ | Resonant Frequency GHz |
|---|---|---|
|  | 75 | $4.778 + j0.0258$ |
|  | 85 | $4.496 + j0.0204$ |
|  | $\varepsilon_{r_1} = 85$ $\varepsilon_{r_2} = 75$ | $4.635 + j0.0233$ |
|  | $\varepsilon_{r_1} = 85$ $\varepsilon_{r_2} = 75$ | $4.627 + j0.0228$ |

**TABLE 1** Convergence Data for Geometry 1

| | Resonant Frequency (GHz) | | |
|---|---|---|---|
| $m_x \times m_y$ | $m_z = 2$ | $m_z = 3$ | $m_z = 4$ |
| $4 \times 4$ | $4.66293 + j0.0217900$ | $4.66663 + j0.0217735$ | $4.65718 + j0.0214628$ |
| $6 \times 6$ | $4.63256 + j0.0223469$ | $4.65815 + j0.0229616$ | $4.65994 + j0.0229538$ |
| $8 \times 8$ | $4.61133 + j0.0221760$ | $4.64479 + j0.0230251$ | $4.65216 + j0.0231809$ |
| $10 \times 10$ | $4.59942 + j0.0220200$ | $4.63556 + j0.0229494$ | $4.64573 + j0.0231873$ |

**TABLE 2** Comparison of Theoretical and Experimental Resonant Frequencies

| Geometry | $F_{\text{res}}$ (GHz) (Exp.) [4] | $F_{\text{res}}$ (GHz) (FWM) [17] | $F_{\text{res}}$ (GHz) (DWM) [4] | Error (% $F_{\text{res}}$) (DWM) [4] | $F_{\text{res}}$ (GHz) (FCNP) | Error (% $F_{\text{res}}$) (FCNP) |
|---|---|---|---|---|---|---|
| 1 | $4.673 + j0.0246$ | — | $4.346 + j0.0169$ | $-7.0$ | $4.646 + j0.0232$ | $-0.58$ |
| 2 | $6.322 + j0.1109$ | — | $5.934 + j0.0783$ | $-6.1$ | $6.278 + j0.0968$ | $-0.69$ |
| 3 | $5.684 + j0.0902$ | $5.649 + j0.0766$ | $5.337 + j0.0606$ | $-6.1$ | $5.650 + j0.0762$ | $-0.6$ |

**TABLE 4   Fundamental Resonant Frequency for an Inhomogeneous Resonator Comprised of Two Homogeneous Sections with Greatly Different Permittivities**

| Permittivity | Resonant Frequency (GHz) |
|---|---|
| $\varepsilon_{r_1} = 60$ $\varepsilon_{r_2} = 30$ | $5.316 + j0.0617$ |
| $\varepsilon_{r_1} = 70$ $\varepsilon_{r_2} = 20$ | $5.395 + j0.0518$ |
| $\varepsilon_{r_1} = (70, -0.05)$ $\varepsilon_{r_2} = (20, -0.014)$ | $5.395 + j0.0537$ |
| $\varepsilon_{r_1} = (70, -1)$ $\varepsilon_{r_2} = (20, -0.285)$ | $5.394 + j0.0891$ |

specific background environment into which the dielectric resonator (or antenna) is placed. Here, we have concentrated on the suitability of the numerical method for inhomogeneous resonators having high permittivity, rather than specific resonator or antenna environments.

## V. CONCLUSION

Inhomogeneous dielectric resonators are finding increasing use in microwave/millimeter-wave circuits. The face-centered node-point technique discussed here is a relatively simple (based on pulse functions) full-wave method that provides a stable algorithm for computing the resonance frequencies of inhomogeneous dielectric resonators having high permittivity. The method is accurate, and does not lead to ill-conditioned matrices such as arise from conventional numerical solutions of the governing volume integral equations in the high-permittivity case. Numerical results for homogeneous dielectric resonators have been compared with other theoretical and experimental results to validate the method, and new results for multilayer dielectric resonators have been provided.

## REFERENCES

1. C.C. Su, A procedure for solving the electric field integral equation for a dielectric scatterer with a large permittivity using face-centered node points, IEEE Trans Microwave Theory Tech 39 (1991), 1043–1048.
2. C.C. Su, The three-dimensional algorithm of solving the electric field integral equation using face-centered node points, conjugate gradient method, and FFT, IEEE Trans Microwave Theory Tech 41 (1993), 510–515.
3. R.R. Bonetti and A.E. Atia, Design of cylindrical dielectric resonators in inhomogeneous media, IEEE Trans Microwave Theory Tech MTT-29 (1981).
4. R. Kumar and A. Ittipiboon, Theoretical and experimental investigations on rectangular dielectric resonator antennas, IEEE Trans Antennas Propagat 45 (1997), 1348–1356.
5. B. Henry, A. Petosa, Y.M.M. Antar, and G.A. Morin, Mutual coupling between rectangular multisegment dielectric resonator antennas, Microwave Opt Technol Lett 21 (1999), 46–48.
6. K.M. Luk, K.W. Leung, and K.Y. Chow, Bandwidth and gain enhancement of a dielectric resonator antenna with the use of a stacking element, Microwave Opt Technol Lett 14 (1997), 215–217.
7. M.J. Hagmann, O.P. Gandhi, and C.H. Durney, Upper bound on cell size for moment-method solutions, IEEE Trans Microwave Theory Tech MTT-25 (1977), 831–832.
8. M.J. Hagman, Comments on "Limitations of the cubical block model of man in calculating SAR distributions," IEEE Trans Microwave Theory Tech MTT-33 (1985), 347–348.
9. H. Massoudi, C.H. Durney, and M.F. Iskander, Limitations of the cubical block model of man in calculating SAR distributions, IEEE Trans Microwave Theory Tech MTT-32 (1984), 746–752.
10. D.T. Borup, D.M. Sullivan, and O.P. Ganghi, Comparison of the FFT conjugate gradient method and the finite-difference time-domain method for the 2D absorption problem, IEEE Trans Microwave Theory Tech MTT-35 (1987), 383–395.
11. A.F. Peterson and R. Mittra, Convergence of the conjugate method when applied to matrix equations representing electromagnetic scattering problems, IEEE Trans Microwave Theory Tech MTT-35 (1986), 1447–1454.
12. D.H. Schaubert, D.R. Wilton, and A.W. Glisson, A tetrahedral modeling method for electromagnetic scattering by arbitrarily shaped inhomogeneous dielectric bodies, IEEE Trans Antennas Propagat AP-32 (1984), 77–85.
13. C.C. Su, Calculation of electromagnetic scattering from a dielectric cylinder using the conjugate gradient method and FFT, IEEE Trans Antennas Propagat AP-35 (1987), 1418–1425.
14. M.J. Hagmann and R.L. Levin, Accuracy of block models for evaluation of the deposition of energy by electromagnetic fields, IEEE Trans Microwave Theory Tech MTT-34 (1986), 653–658.
15. C.T. Tsai, M. Massoudi, C.H. Durney, and M.F. Iskander, A procedure for calculating fields inside arbitrarily shaped, inhomogeneous dielectric bodies using linear basis functions with the moment method, IEEE Trans Microwave Theory Tech MTT-34 (1986), 1131–1138.
16. K.A. Walters, Face-centered point-matching method of moments with applications to scattering and resonance problems, M.S.E.E. thesis, University of Wisconsin–Milwaukee, Dec. 2000.
17. G.W. Hanson and S.L. Lin, An efficient full-wave method for analysis of dielectric resonators possessing separable geometries immersed in inhomogeneous media, IEEE Trans Microwave Theory Tech 48 (2000), 84–92.

# DEPENDENCE OF OPTICAL POWER CONFINEMENT ON CORE/CLADDING CHIRALITIES IN CHIROFIBERS

**P. K. Choudhury[1] and T. Yoshino[2]**
[1] Satellite Venture Business Laboratory
Faculty of Engineering
Gunma University
Kiryu 376-8515, Gunma, Japan
[2] Department of Electronic Engineering
Faculty of Engineering
Gunma University
Kiryu 376-8515, Gunma, Japan

**ABSTRACT:** *An analytical study of the optical power confinement of a chirofiber is presented. Using Maxwell's field equations and considering the cases of meridional and skew modes, variation of the power confinement is presented in two events, viz. 1) with the change in cladding chirality (for fixed values of core chirality), and 2) with the change in core chirality (for fixed values of cladding chirality). Studies are made for two different fiber core diameters, and it is found that, in general, the power confinement in the core section reduces with the increase in its chirality admittance. Further, the amount of transmitted power increases with the mode index. However, as the core cross-sectional size increases, the skew modes present almost similar behavior, and the power transported by them is much higher as compared to that by the meridional modes. Thus, the skew modes in such chirofibers with a little larger size present an event close to degeneracy, which is useful in integrated-optic applications and optical-communication systems. © 2002 John Wiley & Sons, Inc. Microwave Opt Technol Lett 32: 359–364, 2002.*